



# Modeling Pancreatic Cancer Dynamics with Immunotherapy

Xiaochuan Hu<sup>1,2</sup> · Guoyi Ke<sup>1,3</sup> · Sophia R.-J. Jang<sup>1</sup>

Received: 28 April 2018 / Accepted: 22 February 2019 / Published online: 6 March 2019  
© Society for Mathematical Biology 2019

## Abstract

We develop a mathematical model of pancreatic cancer that includes pancreatic cancer cells, pancreatic stellate cells, effector cells and tumor-promoting and tumor-suppressing cytokines to investigate the effects of immunotherapies on patient survival. The model is first validated using the survival data of two clinical trials. Local sensitivity analysis of the parameters indicates there exists a critical activation rate of pro-tumor cytokines beyond which the cancer can be eradicated if four adoptive transfers of immune cells are applied. Optimal control theory is explored as a potential tool for searching the best adoptive cellular immunotherapies. Combined immunotherapies between adoptive ex vivo expanded immune cells and TGF- $\beta$  inhibition by siRNA treatments are investigated. This study concludes that mono-immunotherapy is unlikely to control the pancreatic cancer and combined immunotherapies between anti-TGF- $\beta$  and adoptive transfers of immune cells can prolong patient survival. We show through numerical explorations that how these two types of immunotherapies are scheduled is important to survival. Applying TGF- $\beta$  inhibition first followed by adoptive immune cell transfers can yield better survival outcomes.

**Keywords** Pancreatic cancer · Immunotherapy · Cytokine · Ordinary differential equations

**Mathematics Subject Classification** 92D25 · 92B05

---

✉ Sophia R.-J. Jang  
sophia.jang@ttu.edu

<sup>1</sup> Department of Mathematics and Statistics, Texas Tech University, Lubbock, TX 79409-1042, USA

<sup>2</sup> Present Address: Department of Mathematics and Statistics, University of the Incarnate Word, San Antonio, TX 78209, USA

<sup>3</sup> Present Address: Department of Mathematics and Physical Sciences, Louisiana State University of Alexandria, Alexandria, LA 71302, USA

## 1 Introduction

The pancreas is a glandular organ behind the stomach that secretes several important hormones and enzymes. When the organ loses homeostasis, uncontrolled proliferations occur and pancreatic cancer arises. There are several types of pancreatic cancer, including pancreatic ductal adenocarcinoma (PDA), which is the most common type of pancreatic cancer. In the USA, the one-year pancreatic cancer survival rate is about 25% and the five-year survival rate is  $< 5\%$  (Ellermeier et al. 2013; Hariharan et al. 2008; Louzoun et al. 2014). Treatments of pancreatic cancer consist of surgery, radiotherapy, chemotherapy or a combination of these. The treatment options are largely based on cancer stages, and currently, surgery is the only treatment that can cure localized pancreatic cancer. For patients with metastatic pancreatic cancer, the survival time is only about 3–4 months. With gemcitabine, a common chemotherapy for pancreatic cancer, the life of advanced pancreatic cancer patients may be extended for up to 6 months (Niu et al. 2013).

The immune system has the ability to detect cancer cells by the antigens expressed on those cells. The tumor immunosurveillance hypothesis states that the immune system is capable of inhibiting the growth of very small tumors and eliminating them before they become clinically evident (Weinberg 2013). However, there are numerous ways that cancer cells can escape immune surveillance. For example, cancer cells can reduce the expression of tumor antigens on their surface, making it harder for the immune system to detect them. Tumor cells may express proteins on their surface that induce immune cell inactivation and may also induce cells in the tumor microenvironment to release substances that suppress immune responses and promote tumor cell proliferation and survival (Hanahan and Weinberg 2011; Weinberg 2013).

The cancer microenvironment is very complex and continuously changing. Mathematical modeling of cancer and the immune system therefore becomes a powerful tool for developing improved treatment strategies and for predicting cancer prognosis. One of the first mathematical models on tumor effector cells interactions is a two-dimensional system of ordinary differential equations proposed by Kuznetsov et al. (1994). Their stability and bifurcation analysis helps to determine critical parameters that are important for tumor progression and eradication. A pioneer mathematical model to investigate the role of cytokines, specifically IL-2, on tumor progression is developed by Kirschner and Panetta (1998). They study the effect of IL-2 and cytotoxic T cells on tumor-immune dynamics and conclude that it is possible to eradicate tumor cells by injection of IL-2 alone. In these two models (Kuznetsov et al. 1994; Kirschner and Panetta 1998), cell populations and cytokines are assumed to be homogeneously mixed in space. In addition, the tumor in the tumor-immune systems proposed is assumed for generic cancer.

Pancreatic cancer is the fourth most common cause of cancer-related death worldwide. It has extremely poor prognosis and is characterized by early metastasis and resistance to chemotherapy and radiation (Ellermeier et al. 2013). It has been estimated recently that by 2030, PDA will be the second most common cause of cancer-related mortality, indicating the limited impact of cancer therapy research to date on the clinical course of the disease (Maloney et al. 2017). In order to better understand the pancreatic cancer prognosis and mechanisms behind cancer progression, several

mathematical models have been developed recently. The pioneer work of Louzoun et al. (2014) uses a mathematical model of nonlinear ordinary differential equations to study the disease and provides a starting point for identifying optimal nodes for intervention against the cancer. In this model, pro-inflammatory macrophages and anti-inflammatory macrophages are explicitly built into the interaction in which the tumor is able to induce polarization of pro-inflammatory macrophages into anti-inflammatory macrophages that promotes expansion of myeloid-derived suppressor cells which eventually block the killing of cancer cells by cytotoxic T cells. Treatments such as TGF- $\beta$  silencing and immune activation are applied by reducing several critical parameter values in the model. Comparing the numerical results of the model of no treatment with the model of various treatments, it is concluded that there is a window of opportunity for successful treatments (Louzoun et al. 2014).

Using ordinary differential equations, Li and Xu (2016) propose a model of interaction between pancreatic cancer and immune system with pulsed immunotherapies. The study confirms that immunotherapy offers a better prognosis for pancreatic cancer patients than that of no immunotherapy. Recently, He and Xu (2017) extend the model of Li and Xu (2016) by considering regulatory T cells (Tregs). It has been reported that Tregs modulate the function of effector cells rendering them unable to perform their cytotoxic activity effectively, leading to a weak or nonexistent immune response to tumor cells (He and Xu 2017). Cyclophosphamide (CTX) is a Treg inhibitory therapy, and it is known that low doses of CTX can boost anti-tumor activity by reducing the number and activity of Tregs. Using numerical simulations, He and Xu (2017) conclude that a combination of treatments of immunotherapy and CTX can increase the overall survival of pancreatic cancer patients. More recently, Friedman and Hao (2017) build a model of partial differential equations by incorporating exosomes in the interaction. Their study shows that the size of the pancreatic cancer can be determined by the measurement of specific miRNAs in exosomes.

The research by Louzoun et al. (2014), Li and Xu (2016) and He and Xu (2017) on pancreatic cancer provides important insights on tumor evolution and possible control mechanisms, where quasi-steady-state approximations are used in their investigations and important biological conclusions are based on the reduced models. In particular, cytokines productions are assumed to be linearly proportional to the appropriate cell populations (Louzoun et al. 2014; Li and Xu 2016; He and Xu 2017). This assumption is a very rough estimate since communication between cells via cytokines is very complex. In this work, we adopt Michaelis–Menten kinetics as in Kirschner and Panetta (1998), Arciero et al. (2004) and Eftimie et al. (2010) to model cytokine productions. We group effector cells of CD8<sup>+</sup> T cells and natural killer cells as a single compartment. The cytokines are separated into two groups, one that is tumor promoting and the other that is tumor suppressing. The role of TGF- $\beta$  on promoting tumor growth by inhibiting anti-tumor activity of effector cells and deactivating proliferations of these cells is well established (Ellermeier et al. 2013; Gold 1999; Nam et al. 2008). Cytokines such as IL-6 can also reduce the ability of effector cells (Xue et al. 2016). Further, cytokines such as IFN- $\gamma$  and IL-2 can help effector cells combat cancer cells by activating effector cells. These cytokines can increase effector cell production and inhibit communication between pancreatic cancer cells and their microenvironment (Louzoun et al. 2014).

The resulting model is a five-dimensional system of nonlinear ordinary differential equations, and we investigate the system directly without using quasi-steady-state approximations. To validate the proposed system, we first numerically simulate the model without any immunotherapies using three different immune strengths. We then apply pulsed treatments of immunotherapy to patients with various immune levels. Our numerical results agree with the clinical data given by Niu et al. (2013) in terms of survival time, where the median overall survival in Niu et al. is 7 and 13 months for those patients who underwent cryotherapy and cryo-immunotherapy, respectively. We then compute the maximal percentage of change that each parameter can be varied for which the survival time is within the range of the data set described by Niu et al. In addition, we apply our baseline parameter values with randomly chosen tumor growth rates to 100 numerically generated patients to simulate and validate the model with respect to the percentage survival data of Chung et al. (2014). Once the model is validated, we apply siRNA treatments to reduce TGF- $\beta$  production and compare anti-TGF- $\beta$  treatments with injections of effector cells. We use optimal control theory as a potential tool for searching the best treatment strategy with adoptive transfers of immune cells. In silico experiments using baseline parameter values are performed to explore different combined strategies of anti-TGF- $\beta$  and adoptive transfers of immune cells for better survival outcomes.

The remainder of this manuscript is organized as follows. In Sect. 2, we develop and validate the proposed model. In Sect. 3, the model with TGF- $\beta$  inhibition using siRNA treatments is introduced and optimal control theory is applied to provide best treatment strategies in terms of doses and schedules of the adoptive transfers of immune cells. Numerical explorations with combined immunotherapies are also given in Sect. 3. The final section provides conclusions and directions for possible future work.

## 2 The Proposed Model and Model Validation

The most prevalent type of pancreatic cancer is pancreatic ductal adenocarcinoma (PDA), which is investigated by Louzoun et al. (2014), Li and Xu (2016) and He and Xu (2017) and is the subject of this study as well. Pancreatic cancer cells (PCCs) of the pancreatic ductal adenocarcinoma are epithelial cells, and pancreatic stellate cells (PSCs) are fibroblast cells representing a major component of the tumor stroma. It is widely recognized that pancreatic stellate cells play important roles in the evolution of pancreatic cancers (Bachem et al. 2008; Mace et al. 2013). In particular, PSCs can act to enhance the growth and metastatic properties of PCCs and have been suggested as having an immune modulatory potential (Louzoun et al. 2014). PSCs also produce cytokines including TGF- $\beta$  and IL-6 which in turn promote an immunosuppressive microenvironment (Ellermeier et al. 2013; Gaspar et al. 2007; Louzoun et al. 2014; Mace et al. 2013).

We first briefly describe the assumptions made in the two models proposed by Louzoun et al. (2014) and Li and Xu (2016). The unit of cells and cytokines in Louzoun et al. are number of cells per ml and mM, respectively, while their units in Li and Xu (2016) are number of cells and ng per ml, respectively. In Louzoun et al. (2014), production of effector cells is constantly proportional to the tumor-suppressing cytokines

but is inhibited by tumor-promoting cytokines. In particular, a single compartment is used to include all types of effector cells. In Li and Xu (2016), the immune system consists of three compartments, namely the  $CD8^+$  T cells, natural killer (NK) cells and helper T cells, where both  $CD8^+$  T cells and NK cells are able to kill tumor cells. Moreover, the production of each of these immune cells is simulated by tumor-suppressing cytokines and is modeled by the Michaelis–Menten form, but there is no inhibition on tumor killing by pro-tumor cytokines. The killing rate of  $CD8^+$  T cells on PCCs in Li and Xu (2016) is modeled by a form adopted from de Pillis et al. (2008) while the killing of NK cells on PCCs follows a mass action. The killing of tumor by effector cells in Louzoun et al. (2014) is modeled by a mass action, and the rate is inhibited by tumor-supporting cytokines. The systems studied by Louzoun et al. (2014), Li and Xu (2016) and He and Xu (2017) have the same growth rate for PSCs, while the growth rates for PCCs are different. The PCCs follow a logistic growth in Li and Xu (2016) and He and Xu (2017), and a universal law is used in Louzoun et al. (2014).

In the next subsection, we develop the proposed model. The selection of parameter values is discussed in Sect. 2.2. The proposed model is validated in Sect. 2.3 using numerical simulations by comparing patients' survival time with the clinical data presented in Niu et al. (2013) and in Chung et al. (2014).

## 2.1 Model Development

The state variables consist of PSCs, PCCs, effector cells and two types of cytokines and are summarized as follows:

- $x$ : pancreatic cancer cell (PCC) population
- $y$ : pancreatic stellate cell (PSC) population
- $z$ : effector cells, including  $CD8^+$  T cells and NK cells
- $w$ : concentration of tumor-promoting cytokines, including TGF- $\beta$  and IL-6
- $v$ : concentration of tumor-suppressing cytokines, including IFN- $\gamma$  and IL-2.

The time unit is a day, the unit of cell populations is the number of cells, and the concentration of cytokines is  $\text{pg ml}^{-1}$ . Similar to the research carried out by Louzoun et al. (2014), Li and Xu (2016) and He and Xu (2017), we assume that cell populations and cytokines are distributed homogeneously in space. In the absence of the immune system, PCCs grow logistically with intrinsic growth rate  $r_1$  and carrying capacity  $1/b_1$ . This logistic growth assumption is assumed in many cancer models (Kuznetsov et al. 1994; Kirschner and Panetta 1998; Arciero et al. 2004; de Pillis et al. 2005; Anderson et al. 2015; Li and Xu 2016; He and Xu 2017; Hu and Jang 2018a). In addition, PSCs promote proliferation of PCCs with a constant rate  $\beta_1$  and PCCs are killed by effector cells with the killing rate being inhibited by tumor-promoting cytokines. Therefore, the rate of change in PCCs is given by

$$x' = (r_1 + \beta_1 y)x(1 - b_1 x) - \frac{\delta_1 x z}{m_1 + w}, \quad (1)$$

where  $\delta_1$  is the maximum tumor killing rate and  $m_1$  determines the concentration of tumor-promoting cytokines at which their inhibition becomes important.

As in Louzoun et al. (2014), Li and Xu (2016) and He and Xu (2017), PSCs grow logistically with intrinsic growth rate  $r_2$ , carrying capacity  $1/b_2$  and natural death rate  $\mu_2$ . Further, tumor-promoting cytokines stimulate PSC proliferations with a maximum rate  $\beta_2$  and a half-saturation constant  $k_2$ . That is, the equation for PSCs is given as

$$y' = \left( r_2 + \frac{\beta_2 w}{k_2 + w} \right) y(1 - b_2 y) - \mu_2 y. \quad (2)$$

Effector cells are produced naturally with a rate  $r_3$  and die at a constant rate  $\mu_3$ . Due to cancer cells, the production of effector cells is also activated by the communication between effector cells and tumor-suppressing cytokines. This additional production has a maximum rate  $\beta_3$  and a half-saturation constant  $k_3$ . However, tumor-promoting cytokines are able to inhibit this proliferation with a constant  $m_3$  that determines when the concentration of tumor-promoting cytokines becomes important. This inhibition is not incorporated in the models studied by Li and Xu (2016) and He and Xu (2017). The corresponding equation for effector cells is

$$z' = \frac{\beta_3 z v}{(k_3 + v)(m_3 + w)} - \mu_3 z + r_3. \quad (3)$$

The production of tumor-promoting cytokines comes from the interaction between cancer cells and effector cells and is modeled by a Michaelis–Menten form to account for the self-limiting production of the cytokines. This particular form is used in several cancer–immune system studies such as Kirschner and Panetta (1998), Arciero et al. (2004) and Eftimie et al. (2010). The decay rate is denoted by  $\mu_4$ , and the production of tumor-promoting cytokines is augmented through communication between PCCs and the tumor stromal PSCs with a maximum rate  $r_4$  (Kozono et al. 2013). This extra proliferation is inhibited by the tumor-suppressing cytokines with a constant  $m_4$ , and the equation for  $w$  is

$$w' = \frac{\beta_4 x z}{k_4 + x} - \mu_4 w + \frac{r_4 x y}{m_4 + v}. \quad (4)$$

The last expression in the equation of pro-tumor cytokines is not modeled in Louzoun et al. (2014), Li and Xu (2016) or He and Xu (2017). The equation for tumor-suppressing cytokines is similar to the tumor-promoting cytokines without the augmentation term and is given by

$$v' = \frac{\beta_5 x z}{k_5 + x} - \mu_5 v, \quad (5)$$

where  $\beta_5$  is the maximum production rate,  $k_5$  is the half-saturation constant and  $\mu_5$  is the decay rate.

Putting all of these together, the interaction between PCCs, PSCs and the immune system is described by

$$\begin{cases} x' = (r_1 + \beta_1 y)x(1 - b_1 x) - \frac{\delta_1 xz}{m_1 + w} \\ y' = (r_2 + \frac{\beta_2 w}{k_2 + w})y(1 - b_2 y) - \mu_2 y \\ z' = \frac{\beta_3 zv}{(k_3 + v)(m_3 + w)} - \mu_3 z + r_3 \\ w' = \frac{\beta_4 xz}{k_4 + x} - \mu_4 w + \frac{r_4 xy}{m_4 + v} \\ v' = \frac{\beta_5 xz}{k_5 + x} - \mu_5 v \\ x(0) > 0, y(0) > 0, z(0) \geq 0, w(0) \geq 0, v(0) \geq 0. \end{cases} \tag{6}$$

In the following, we study system (6) without using quasi-steady-state approximations.

It is clear that solutions of (6) exist and remain nonnegative on  $[0, \infty)$ . Moreover, the solution is unique if an initial condition is specified. The parameters and their biological interpretations are summarized in Table 1.

Once the model is constructed, we proceed to study the tumor–immune interaction numerically. The model (6) has 23 parameters and many nonlinear reaction terms. In the next subsection, we discuss how the parameter values will be selected.

### 2.2 Parameter Values and Their Sources

The cancer–immune system is a very complicated biological network involving numerous positive and negative feedbacks between various receptors, ligands and cells. Several of the cytokines can also change their functions during different stages of cancer progression. In addition to these, different patients of the same cancer type are likely to have different immune response, tumor load, aggressiveness of tumor and various cytokine levels. There are insufficient data available to parameterize model (6), and therefore, parameter values are taken from multiple sources.

Several of the numerical values are taken from Li and Xu (2016) directly since they also model pancreatic cancer. In particular, the values of  $r_1$ ,  $\beta_1$  and  $b_1$  are from Li and Xu (2016) where their values of  $r_1$  and  $b_1$  are due to de Pillis et al. (2008) with some variants to account for the aggression of the pancreatic cancer. The tumor growth rate  $r_1$  and carrying capacity  $1/b_1$  in de Pillis et al. (2008) were estimated from the data in Diefenbach et al. (2001) using least squares goodness of fit. The value of  $\beta_1$  in Li and Xu (2016) comes from Louzoun et al. (2014) for studying PDA patients survival, where the value in Louzoun et al. (2014) is estimated to fit with the survival percentage of Ellermeier et al. (2013) for an orthotopic Panc02 mouse model of pancreatic cancer. The tumor killing rate  $\delta_1$  is 5 in de Pillis et al. (2008) and 1 in Kirschner and Panetta (1998). We use the value 0.96 and it is  $5 \times 10^{-3}$  in Li and Xu

**Table 1** Parameters and their biological meanings

Parameter	Description
$r_1$	Intrinsic growth rate of PCC
$b_1$	Reciprocal of carrying capacity of PCC
$\beta_1$	Maximum activation rate of PCC due to PSC
$m_1$	Concentration of tumor-promoting cytokines at half-maximum for inhibition
$\delta_1$	Maximum killing rate of PCC by effector cells
$r_2$	Intrinsic growth rate of PSC
$\beta_2$	Maximum activation rate of PSC due to tumor-promoting cytokines
$k_2$	Half-saturation constant of PSC activation rate
$b_2$	Reciprocal of carrying capacity of PSC
$\mu_2$	Natural death rate of PSC
$\beta_3$	Maximum production rate of effector cells
$k_3$	Half-saturation constant of production rate of effector cells
$m_3$	Concentration of tumor-promoting cytokines at half-maximum for inhibition
$r_3$	Natural proliferation rate of effector cells
$\mu_3$	Apoptosis rate of effector cells
$\beta_4$	Maximum production rate of tumor-promoting cytokines
$k_4$	Half-saturation constant of maximum production rate of pro-tumor cytokines
$\mu_4$	Decay rate of tumor-promoting cytokines
$r_4$	Maximum production rate of tumor-promoting cytokines due to PSC
$m_4$	Concentration of tumor-suppressing cytokines at half-maximum for inhibition
$\beta_5$	Maximum production rate of tumor-suppressing cytokines
$k_5$	Half-saturation constant of maximum production rate of anti-tumor cytokines
$\mu_5$	Decay rate of tumor-suppressing cytokines

(2016). The  $\delta_1$  value chosen here is larger than Li and Xu (2016) since inhibition of tumor killing by pro-tumor cytokines is not considered in Li and Xu (2016). There are no data available for  $m_1$  for the cancer type, and we adopt  $10^8$  from Eftimie et al. (2010) for a mouse melanoma model. One can see from Sect. 2.3 that increasing  $m_1$  by up to 3000% or decreasing it by up to 90% from the baseline value the survival time remains consistent with the clinic data given in Niu et al. (2013).

Since the equation of PSCs is unchanged from the previous three pancreatic cancer models (Louzoun et al. 2014; Li and Xu 2016; He and Xu 2017), the parameter values  $r_2$ ,  $\beta_2$ ,  $k_2$ ,  $b_2$  and  $\mu_2$  for the equation of PSCs are based on Li and Xu (2016), while their values are estimated from Louzoun et al. (2014) and the values in Louzoun et al. (2014) are stated as estimated to fit in the survival percentage of a Panc02 mouse model. For the effector cell equation, both  $r_3$  and  $\mu_3$  values follow from Li and Xu (2016). The loss rate  $\mu_3$  of effector cells used in Li and Xu (2016) is adopted from de Pillis et al. (2008), while the value of de Pillis et al. (2008) is taken from Kuznetsov et al. (1994) using a nonlinear least squares fitting to mice data given by Siu et al. (1986). The value of  $r_3$  in Li and Xu (2016) is stated as estimated to fit in the survival



data of Niu et al. (2013). The value of  $\beta_3$  is adopted from Kirschner and Panetta (1998), while  $k_3$  and  $m_3$  are from Eftimie et al. (2010).

Parameter values involving cytokines are largely taken from a mouse melanoma model of Eftimie et al. (2010) where the decay rates  $\mu_i$  in Eftimie et al. (2010),  $i = 4, 5$ , are calculated using the half-life of cytokines. The production rates  $\beta_i$ ,  $i = 4, 5$ , of cytokines are estimated from Eftimie et al. (2010) where they are stated as “guess” in Eftimie et al. (2010) and our values are larger than theirs but of the same order. There is an augmented term in the equation for pro-tumor cytokines that models the stimulation from cross talk between PSCs and PCCs, which is not modeled in the previous studies Li and Xu (2016); Xu and Wang (2015); Louzoun et al. (2014). Therefore, the two parameters  $r_4$  and  $m_4$  in this expression are chosen to fit with the survival data of Niu et al. (2013).

Baseline parameter values are presented in Table 2, which will be used to validate model (6). In summary, if a reference is cited for a particular parameter, it means that the value is taken from the cited reference directly without any modification. In contrast, “estimated” means that we cannot find those values in the existing literature and we select the values to match with the clinical survival data given by Niu et al. (2013). When “estimated from” a reference is specified for a parameter value, it indicates that the original parameter value is available but may not be suitable for the model of pancreatic cancer and variation is taken.

## 2.3 Model Validation

In this section, we validate model (6) using two clinical survival data of pancreatic cancer patients based on the parameter values given in Table 2. The survival data of Niu et al. (2013) are used in Sect. 2.3.1, and the data of Chung et al. (2014) are applied to validate model (6) in Sect. 2.3.2. In addition, we vary each individual parameter in “Appendix” to obtain the maximum percentage that a parameter can be varied from the baseline value for which the clinical survival data in Niu et al. (2013) are matched.

### 2.3.1 Validation Through the Survival Data of Niu et al.

The study of Niu et al. (2013) is to assess retrospectively the effect of different treatment methods, including cryotherapy (31 patients), cryo-immunotherapy (36 patients), immunotherapy (17 patients) and chemotherapy (22 patients) on patient’s survival. According to Niu et al. (2013), the overall survival for the patients in the cryo-immunotherapy group is better than for the patients in the cryotherapy group and cryotherapy is safe to perform.

Cryotherapy is the use of extreme cold produced by liquid nitrogen or argon gas to destroy abnormal tissue (Luo et al. 2016), and cryo-immunotherapy is the treatment by performing cryotherapy first followed by immunotherapy. It is stated in Niu et al. (2013) that the advantage of cryotherapy is the cryo-immunologic response, which is an anti-tumor immune response triggered by the natural absorption of the malignant tissue. In addition, cryotherapy is considered as a palliative therapy. Therefore, cryotherapy is not explicitly modeled in (6), but we apply the data of patients who

**Table 2** Baseline parameter values and their sources

Parameter	Value	Reference
$r_1$	$1.95 \times 10^{-2} \text{ day}^{-1}$	Li and Xu (2016)
$b_1$	$1.02 \times 10^{-11} \text{ cell}^{-1}$	Li and Xu (2016)
$\beta_1$	$1.95 \times 1.7857 \times 10^{-12} (\text{cell} \cdot \text{day})^{-1}$	Li and Xu (2016)
$m_1$	$10^8 \text{ pg} \cdot \text{ml}^{-1}$	Eftimie et al. (2010)
$\delta_1$	$0.96 \text{ pg} \cdot \text{ml}^{-1} \cdot \text{cell}^{-1} \cdot \text{day}^{-1}$	Estimated from Kirschner and Panetta (1998)
$r_2$	$1.95 \times 10^{-3} \text{ day}^{-1}$	Li and Xu (2016)
$\beta_2$	$0.125 \text{ day}^{-1}$	Li and Xu (2016)
$k_2$	$5.6 \times 10^{10} \text{ pg} \cdot \text{ml}^{-1}$	Li and Xu (2016)
$b_2$	$1.7857 \times 10^{-9} \text{ cell}^{-1}$	Li and Xu (2016)
$\mu_2$	$0.015 \text{ day}^{-1}$	Li and Xu (2016)
$\beta_3$	$1.245 \times 10^2 \text{ pg} \cdot \text{ml}^{-1} \cdot \text{day}^{-1}$	Kirschner and Panetta (1998)
$k_3$	$2 \times 10^{10} \text{ pg} \cdot \text{ml}^{-1}$	Eftimie et al. (2010)
$m_3$	$10^6 \text{ pg} \cdot \text{ml}^{-1}$	Eftimie et al. (2010)
$r_3$	$3.5 \times 10^3 \text{ cell} \cdot \text{day}^{-1}$	Li and Xu (2016)
$\mu_3$	$2 \times 10^{-2} \text{ day}^{-1}$	Li and Xu (2016)
$\beta_4$	$5.85 \text{ pg} \cdot \text{ml}^{-1} \cdot \text{cell}^{-1} \cdot \text{day}^{-1}$	Estimated from Eftimie et al. (2010)
$k_4$	$10^6 \text{ cell}$	Eftimie et al. (2010)
$\mu_4$	$3.4 \times 10^{-2} \text{ day}^{-1}$	Eftimie et al. (2010)
$r_4$	$1.25 \times 10^4 \text{ pg}^2 \cdot \text{ml}^{-2} \cdot \text{cell}^{-2} \cdot \text{day}^{-1}$	Estimated
$m_4$	$8.9 \times 10^{10} \text{ pg} \cdot \text{ml}^{-1}$	Estimated
$\beta_5$	$7.3 \text{ pg} \cdot \text{ml}^{-1} \cdot \text{cell}^{-1} \cdot \text{day}^{-1}$	Estimated from Eftimie et al. (2010)
$k_5$	$10^6 \text{ cell}$	Eftimie et al. (2010)
$\mu_5$	$3.4 \times 10^{-2} \text{ day}^{-1}$	Eftimie et al. (2010)

underwent cryo-immunotherapy with immunologic results collected after cryotherapy and prior to immunotherapy to simulate model (6). We validate model (6) with respect to the survival times of two groups of patients, namely those with cryotherapy only versus those with cryo-immunotherapy. It is stated in Niu et al. (2013) that the median overall survival times of these two groups of patients are 7 and 13 months, respectively.

To validate model (6), we first simulate the model with no immunotherapy by applying the baseline parameter values given in Table 2 with three different initial immune strengths, namely  $1.3 \times 10^8$ ,  $1.9 \times 10^8$  and  $2.56 \times 10^8$  for  $z(0)$ , which are denoted as the low, median and high immunities, respectively, for simulations. These values are close to those given in Niu et al. (2013) and are of the same order of  $10^8$  for the low and median immunities. The high immunity used here is smaller than the data given in Niu et al. (2013) in order to capture the median overall survival time. The initial tumor loads of PCC and PSC are  $10^9$  and  $5.6 \times 10^6$ , respectively, which are exactly the same as those used by Li and Xu (2016). We next determine

initial conditions for tumor-promoting and suppressing cytokines. According to the data provided in Niu et al. (2013), the concentration of tumor-suppressing cytokines including  $IFN-\gamma$  and  $IL-2$  ranges from 6.91 to 11.89 pg per ml. We use the average value of 9.4 pg per ml, i.e.,  $v(0) = 9.4$  for all simulations. There are no data available for  $TGF-\beta$  in Niu et al. (2013). We adopt the approximated median value of  $TGF-\beta 1$  given by Bellone et al (2006) for  $w(0)$ , where the authors compare various cytokine levels between 65 advanced pancreatic cancer patients with a control group. The  $w(0)$  value is  $5 \times 10^4$  for all simulations. These initial conditions are summarized in Table 3.

Recall that in Louzoun et al. (2014), Li and Xu (2016) and He and Xu (2017), the rates of changes in cytokines are linearly proportional to the appropriate cell populations and quasi- steady-state approximation is used in their analysis and numerical simulations. For our system (6), the productions of cytokines related to cell populations are modeled with more sophistication, and we use the original system to study tumor progression since quasi-steady-state approximations can lead to a loss of many features of the original system as illustrated by Korobeinikov et al. (2016).

Similar to Louzoun et al. (2014), Li and Xu (2016) and He and Xu (2017), the number of cancer cells a human body may withstand is  $2.8 \times 10^{10}$ . When there is no immunotherapy, the survival times as given in the second column of Table 4 are similar to the data provided in Niu et al. (2013). In particular, the survival times for low, median and high immunity are 208, 215 and 220 days, respectively. The survival time is about 1 to 2 weeks longer if a patient has a stronger immune system, and each of these survival times is close to the median overall survival of 7 months given in Niu et al. (2013).

To validate model (6) further, we apply immunotherapy to patients who have received cryotherapy. As described in Niu et al. (2013), the immunotherapy is applied for four times with a 28-day administration period and  $3.36 \times 10^9$  number of cells per injection. Therefore, a dose of  $3.36 \times 10^9$  cells is adopted here that begins on day one with a 28-day administration period for either three or four times to validate

**Table 3** Initial conditions for simulations

Initial conditions	$x(0)$	$y(0)$	$z(0)$	$w(0)$	$v(0)$
Low	$10^9$	$5.6 \times 10^6$	$1.3 \times 10^8$	$5 \times 10^4$	9.4
Median	$10^9$	$5.6 \times 10^6$	$1.9 \times 10^8$	$5 \times 10^4$	9.4
High	$10^9$	$5.6 \times 10^6$	$2.56 \times 10^8$	$5 \times 10^4$	9.4

**Table 4** Simulated survival times (number of days) of cryotherapy and cryo-immunotherapy

Immune strength	No immunotherapy	Immunotherapy	
		3 times	4 times
Low	208	351	385
Median	215	358	387
High	220	363	391

The corresponding survival times for Niu et al. clinical data are 7 and 13 months, respectively

the proposed model. There are three scenarios considered, namely patients with low, median and high immune strengths as described earlier. The corresponding survival times are presented in Table 4. Notice that these survival times are consistent with the clinical data given by Niu et al. (2013) in terms of the median overall survival. In particular, immunotherapy can prolong a patient's life from 7 months with cryotherapy to approximately 13 months with cryo-immunotherapies.

Although the survival data simulated using the baseline parameter values are comparable to the clinical data of Niu et al. (2013) with respect to the median overall survival, the baseline parameter values as described in Sect. 2.2 are taken from different research including different types of cancer. We perform sensitivity analysis by determining the maximum percentage of changes an individual parameter can vary for which the survival time agrees with the clinical data of Niu et al. (2013). The result is given in "Appendix."

### 2.3.2 Validation Through the Survival Data of Chung et al.

There is another set of clinical survival data using *ex vivo* expanded immune cells as a treatment that results from a phase II trial carried out by Chung et al. in Korea (Chung et al. 2014). The trial consists of a small number of 16 patients who have previously undergone gemcitabine-based chemotherapy and refractory. The median overall survival for these 16 patients is 26.6 weeks in which four patients completed ten immunotherapies, four received eight immunotherapies and the rest of the patients took seven immunotherapies (Chung et al. 2014). These patients receive one immunotherapy every week for 5 weeks and then one immunotherapy every other week for up to five additional immunotherapies with  $6.73 \times 10^9$  adoptive cells per therapy. Similar to the study of Louzoun et al. (2014), where 50 patients are simulated using different tumor killing rates based on a geometric sequence between two values to validate their model by matching the survival percentage of an orthotopic Panc02 mouse model of pancreatic cancer of 17 mice, we use 100 simulated patients with different tumor growth rates to compare our numerical results with the clinical data of Chung et al. (2014). We validate model (6) by providing percentage survival of 100 simulated patients that is qualitatively similar to Fig. 2b of Chung et al. (2014).

Recall that the baseline parameter value of tumor growth rate  $r_1$  is taken from Li and Xu (2016) while their value of  $1.95 \times 10^{-2}$  is larger than the one given by de Pillis et al. (2008) of  $2 \times 10^{-3}$ . Since these 16 patients of Chung et al. (2014) are chemotherapy refractory, some of them should have much larger tumor growth rate than the baseline value, while others are smaller. We randomly select 25 tumor growth rates from the interval  $[1.02 \times 10^{-2}, 7.08 \times 10^{-2}]$  to generate survival times for 25 computer-simulated patients of low immunity who take ten immunotherapies. Each dose of the immunotherapy is  $6.73 \times 10^9$  cells with the same scheduling as in Chung et al. (2014) outlined above. The low immunity is used for all simulations since these patients have been treated with chemotherapy and refractory so that their immune system is weaker. Implicitly, we assume each simulated patient is identical except the aggressiveness of the pancreatic cancer is different. We repeat the same procedure for another 25 computer-generated patients who take eight immunotherapies and another 50 simulated patients who receive seven immunotherapies so that the

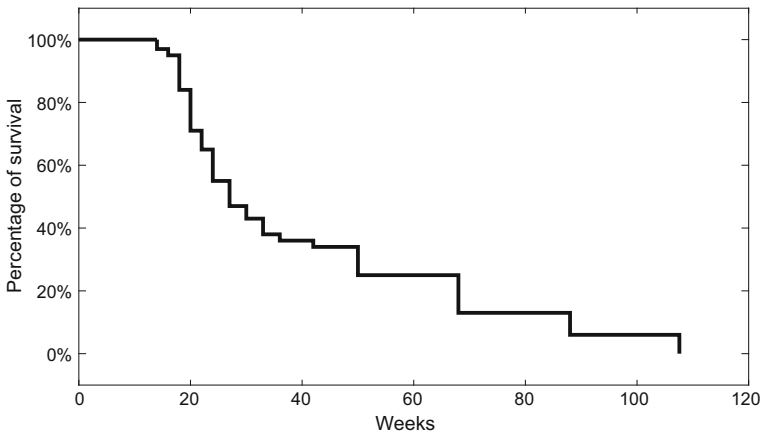


**Fig. 1** Percentage of survival against time for 100 simulated patients of low immunity based on the baseline parameter values of Table 2 with randomly selected tumor growth rates in the range of  $[1.02 \times 10^{-2}, 7.08 \times 10^{-2}]$  is presented. Here, 25 patients receive ten immunotherapies, 25 patients undergo eight therapies, and the remaining 50 patients receive seven immunotherapies. The number of adoptive cells per therapy is  $6.73 \times 10^9$

proportions of patients who undergo seven, eight and ten treatments are the same as in Chung et al. (2014). It is possible that some patients may skip the treatment during the first 5 weeks. For simplicity, we assume the missing of the treatments occurs during the later 10-week period. We then calculate the percentage of survival time of these 100 computer-simulated patients, and the result is presented in Fig. 1. The figure is comparable to Fig. 2b given in Chung et al. (2014). In addition, the median survival of these 100 patients is 27.3 weeks which is close to 26.6 weeks of Chung et al. (2014).

In viewing the above results comparing with two sets of clinical survival data, we can conclude that the proposed model is validated. It is critical to observe that the activation rate  $\beta_4$  of pro-tumor cytokines plays an important role in the outcome of the immunotherapy as indicated in Table 6 where the number of tumor cells is below one if the parameter value is reduced further. This observation will be used to implement treatment strategies discussed in the following section.

### 3 Results on Immunotherapies

Once the model is validated, we proceed to study treatment options that can prolong patients' survival time. We first present the time evolution of PCCs with no immunotherapy, three immunotherapies and four immunotherapies in Fig. 2a using the median strength of immunity and the baseline parameter values of Table 2, where the size of PCCs is rescaled by a common logarithm and the number  $3.36 \times 10^9$  of adopted cells in Niu et al. (2013) is implemented. We see that the first immunotherapy on day one reduces the tumor size drastically. However, successive treatments for an additional two or three times cannot stop the tumor from growing. The PCCs can only be killed by effector cells, while pro-tumor cytokines can inhibit this tumor killing

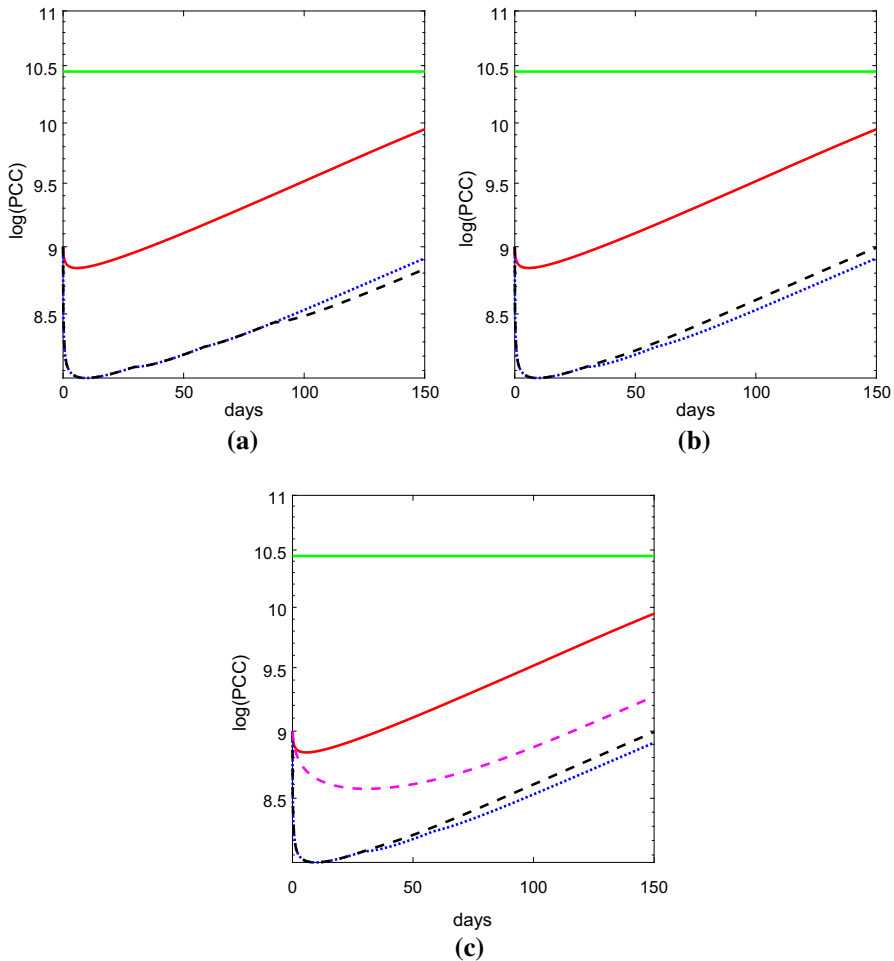


**Fig. 2** Comparing different treatment strategies on tumor size over time using the baseline parameter values in Table 2 and the median immunity in Table 3. All of the red solid lines represent no immunotherapy. **a** Three (blue dotted line) or four (black dashed line) injections of effector cells are applied. **b** Three injections of effector cells (blue dotted line) or one injection of effector cells followed by two siRNA treatments (black dashed line) is applied. **c** A continuous siRNA treatment (magenta dashed line) along with those strategies considered in (b). The parameter values of siRNA treatment are given in (8), and the number of each adoptive cell transfer is  $3.36 \times 10^9$  cells. The break between each successive treatment is 28 days. The PCCs are scaled by a common logarithm, and the top horizontal line is the scaled line of  $2.8 \times 10^{10}$  (Color figure online)

and deactivate production of effector cells. For the first immunotherapy, there are a large number of effector cells at the tumor site which can kill cancer cells and activate pro-tumor cytokines directly. However, there is a delay between activation and production of the tumor-promoting cytokines, and therefore, the first immunotherapy is able to reduce the tumor loads. After the first therapy, there is a period of no treatment. During this period, the tumor grows slowly and the concentration of pro-

tumor cytokines becomes large owing to the effector cells received from the therapy. Therefore, at the subsequent doses of adoptive cells, although the tumor microenvironment is infiltrated with the effector cells, it also contains a large concentration of pro-tumor cytokines so that the effector cells are dysfunctional. As a consequence, only the first immunotherapy is effective in reducing the tumor burden as demonstrated in Fig. 2a.

Tumor-promoting cytokines such as TGF- $\beta$  play a pivotal role in the proliferation of pancreatic cancer cells. Built on model (6), we use siRNA treatments to reduce TGF- $\beta$  production in Sect. 3.1. We apply optimal control theory as a potential tool to devise a best strategy of adoptive cell transfers in terms of dosage and scheduling in Sect. 3.2. As observed earlier that the activation rate of pro-tumor cytokines is important to patients' survival when immunotherapies are applied, we perform in silico experiments with different combinations of treatment strategies in Sect. 3.3 to search for better survival outcomes.

### 3.1 siRNA Treatments

From Fig. 2a, we see that immunotherapy of effector cells on day one has a very good treatment outcome. However, additional injections of effector cells for 2 or 3 more times cannot prevent PCCs from growing. As elaborated earlier, TGF- $\beta$  promotes pancreatic cancer growth and provides a potent immunosuppressive network (Ellermeier et al. 2013). We now consider a different strategy by using siRNA treatments to suppress TGF- $\beta$  production.

RNA interference (RNAi) was first discovered in plants and was not widely noted in animals until Fire et al. (1998) demonstrated that double-stranded RNA (dsRNA) can cause greater suppression of gene expression than single-stranded RNA (ssRNA) in *Caenorhabditis elegans* (Xu and Wang 2015). Small (or short) interfering RNA (siRNA) is the most commonly used RNA interference (RNAi) tool for inducing short-term silencing of protein-coding genes (Xu and Wang 2015). The siRNA treatment involves initial delivery of double-stranded RNA (dsRNA) into tumor cells. The enzyme Dicer then cuts the dsRNA into small segments known as siRNAs. These siRNAs once bounded to the RNA-induced silencing complex (RISC) target TGF- $\beta$  mRNA to prevent TGF- $\beta$  protein from being produced (Lipardi et al. 2001; Holen et al. 2001; Arciero et al. 2004). It is expected that the siRNA treatment should provide a reasonable means of blocking the creation of TGF- $\beta$  gene product and is illustrated in the study by Arciero et al. (2004).

The goal is to incorporate siRNA treatment into model (6) and compare its effects on patients' survival with the method of pulsed immunotherapy explored earlier. We are now ready to describe the model with siRNA treatments. Let  $R$  denote the state variable of total free and bound strands of siRNA. The parameter  $p$  is the proportion of total strands of siRNA that is bound, while  $k$  is the inhibition constant of siRNA. Let  $D_0$  be the constant dose of free siRNA injected to patient per day, and let  $\mu_6$  be the decay rate of siRNA. The model with the treatment by siRNA is given as follows:

$$\left\{ \begin{array}{l} x' = (r_1 + \beta_1 y)x(1 - b_1 x) - \frac{\delta_1 x z}{m_1 + w} \\ y' = (r_2 + \frac{\beta_2 w}{k_2 + w})y(1 - b_2 y) - \mu_2 y \\ z' = \frac{\beta_3 z v}{(k_3 + v)(m_3 + w)} - \mu_3 z + r_3 \\ w' = \frac{\beta_4 x z}{k_4 + \frac{pR}{k}x} - \mu_4 w + \frac{r_4 x y}{m_4 + v} \\ v' = \frac{\beta_5 x z}{k_5 + x} - \mu_5 v \\ R' = D_0 - \mu_6 R \\ x(0) > 0, y(0) > 0, z(0) \geq 0, w(0) \geq 0, v(0) \geq 0, R(0) \geq 0. \end{array} \right. \quad (7)$$

In (7), the equations for PCC, PSC, effectors cells and tumor-suppressing cytokines remain the same as in the corresponding equations of (6). The production of tumor-promoting cytokines is reduced due to bound siRNA that inhibits TGF- $\beta$  production. Model (7) will be studied numerically. This modeling aspect of siRNA treatment is similar to the one used by Arciero et al. (2004), where siRNA treatment can control oscillatory behavior of their model. Louzoun et al. (2014) also discuss anti-TGF- $\beta$  treatment in their study by directly reducing several parameter values involved.

As in Arciero et al. (2004), we adopt the following parameter values

$$D_0 = 5 \times 10^{10} \text{ pg} \cdot \text{ml}^{-1} \text{ per day}, p = 0.9, k = 1 \text{ and } \mu_6 = 0.66. \quad (8)$$

Further, a treatment period of 11 days is used in their numerical investigations (Arciero et al. 2004). Figure 2b presents the size of PCCs over time based on a log 10 scale. The new treatment strategy is as follows. Since the first immunotherapy of  $3.36 \times 10^9$  effector cells on day one is promising, we apply this therapy on day one followed by 28 days of no treatment. On day 30, a constant rate of siRNA is injected for 11 days followed by no treatment for 28 days. A second siRNA treatment is then applied for 11 days afterward. From Fig. 2b, one can see that applying immunotherapy of effector cells thrice performs better than applying it once and with the siRNA treatment twice. This conclusion remains true if the inhibition constant  $k$  is reduced to  $k = 0.001$ . A continuous siRNA treatment started on day one is presented in Fig. 2c which shows that injection of  $3.36 \times 10^9$  effector cells on day one is more effective. Although our modeling methodology of (7) is similar to that of Arciero et al. (2004), our result indicates that injection of effector cells directly is better than blocking TGF- $\beta$  production indirectly.

### 3.2 Optimal Strategy of Adoptive Cell Transfer

As observed from Fig. 2, applying immunotherapies by injecting effector cells three or four times can slow down but cannot stop the tumor from growing. Further, blocking TGF- $\beta$  production after injections of effector cells is not better. In this subsection, we



apply optimal control theory to provide best strategies for treating pancreatic cancer using effector cells.

The optimal control theory has been applied to study cancer immunotherapy by many researchers such as Burden et al. (2004); Castiglione and Piccoli (2007); Khajanchi and Ghosh (2015) and Minelli et al. (2011). In these studies, objective functional may be defined differently depending on the goal of the therapy outcomes. To the best of our knowledge, however, this is the first study applying optimal control theory to investigate immunotherapy for pancreatic cancer.

We first briefly review the research of optimal control of immunotherapy in treating cancer. Burden et al. (2004) propose a model of cancer cells  $T(t)$ , effector cells  $E(t)$  and cytokines  $C(t)$  with optimal control. The control is added to the equation of effector cells using the term  $su(t)$ , where  $s$  denotes strength and  $u$  is the control with  $0 \leq u \leq 1$ .

Their objective functional is given by  $J(u) = \int_0^{t_f} \left( E(t) - T(t) + C(t) - \frac{1}{2}Bu^2(t) \right) dt$ ,  $B > 0$ , and they seek to maximize  $J$  subject to the state equations. Minelli et al. (2011) study a five-dimensional system of ordinary differential equations including effector cells  $E$ , helper cells  $H$ , dendritic cells  $D$ , tumor cells  $T$  and cytokines  $C$  with a control term  $u(t)$  added to the equation of dendritic cells. The objective functional is given

by  $J(u) = \rho T(f_f) + \frac{1}{2} \int_0^{t_f} u^2(t)dt$ , where  $\rho$  is a weighted factor and their goal is to minimize  $J$  subject to the state equations. Notice the term  $t_f$  that appears in the integral of both models denotes the final time. That is, the control is applied over the fixed finite time span  $[0, t_f]$ . More recently, Engelhart et al. (2011) apply optimal control to several published models of tumor-immune interactions. We refer the reader to the studies by Burden et al. (2004), Engelhart et al. (2011), Minelli et al. (2011) and their references for optimal control of immunotherapies on cancer treatments.

We now set up the optimal control problem. Let  $s > 0$  denote the strength of immunotherapy and  $u(t)$  be the bounded control with  $0 \leq u(t) \leq 1$  for  $0 \leq t \leq T$ , where  $[0, T]$  is the fixed time span for treatment. Using the same notation for the state variables as in model (6), the state equations are given by

$$\begin{cases} x' = (r_1 + \beta_1 y)x(1 - b_1 x) - \frac{\delta_1 xz}{m_1 + w} \\ y' = (r_2 + \frac{\beta_2 w}{k_2 + w})y(1 - b_2 y) - \mu_2 y \\ z' = \frac{\beta_3 z v}{(k_3 + v)(m_3 + w)} - \mu_3 z + r_3 + su(t) \\ w' = \frac{\beta_4 xz}{k_4 + x} - \mu_4 w + \frac{r_4 xy}{m_4 + v} \\ v' = \frac{\beta_5 xz}{k_5 + x} - \mu_5 v. \end{cases} \tag{9}$$

The admissible control class is given as

$$U = \{u : u(t) \text{ is piecewise continuous and } 0 \leq u(t) \leq 1 \text{ on } [0, T]\}. \quad (10)$$

The goal of the treatment is to minimize pancreatic cancer cells at the final time and also minimize the pancreatic cancer and pancreatic stellate cells along with the cost or the patient's tolerance associated with the treatment over the whole treatment period  $[0, T]$ . Therefore, the objective functional is given by

$$J(u) = x(T) + \int_0^T (x(t) + y(t) + \frac{1}{2}Au^2(t))dt, \quad (11)$$

where  $A > 0$  is a weighted constant denoting either the cost or the patient's tolerance associated with the treatment. The optimal control problem consists of

$$\min_{u \in U} J(u) \quad (12)$$

subject to the state equations (9). In the objective functional  $J(u)$  given in (11), it is required to minimize PSCs over the treatment period, as PSCs promote growth of PCCs. In addition, we assume identical weights for PCCs and PSCs in  $J(u)$ . We anticipate that decreasing the PSCs can help control the cancer progression.

Clearly the class of all initial conditions with a control  $u \in U$  for the state equations being satisfied on the finite time interval  $[0, T]$  is nonempty. Moreover, solutions of (9) remain nonnegative on  $[0, T]$ . The set of the admissible controls  $U$  is closed and convex and the right-hand side of each of the state equations is continuous, bounded above by the sum of the control, and the state can be written as a linear function of  $u$ . Further, for fixed  $x$  and  $y$ , the integrand of  $J(u)$  is convex on  $U$ . The integrand of  $J(u)$  is convex in  $u$  and is bounded below by  $-C_2 + C_1u^\gamma$  for some  $C_1 > 0$  and  $\gamma = 2 > 1$ . It follows from Fleming and Rishel (1975) that there exists an optimal control for the problem (9)–(12).

Once the existence of an optimal control is shown, we shall solve the optimal control problem (9)–(12) numerically. The problem may be solved either indirectly or directly. The indirect method applies the Pontryagin's maximum principle (Lenhart and Workman 2007) to derive necessary conditions and cast the optimal problem as a two-point boundary value problem. This technique is used in an earlier study by Burden et al. (2004) and Hu and Jang (2018b). However, due to the high nonlinearities associated in the model, we apply the direct collocation method to solve the nonlinear optimal control problem.

In the direct collocation method, the control and the state functions on a time grid are discretized to obtain a nonlinear constrained optimization problem. The time interval is divided into a mesh and the control and/or states are approximated using polynomial approximations or piecewise constant parameterizations in each mesh interval. The cost function formed as an integral term is solved using the method of numerical quadrature integration process. Therefore, the coefficients of the function approximations are treated as optimization variables and the problem is reformulated as a nonlinear programming optimization problem (NLP) which is easier to solve than

the boundary value problem due to the sparsity of the NLP and the many well-known software packages that can be used to solve the problem. In the following simulations, we use the GPOPS-II software, which is integrated with IPOPT NLP solver to handle our optimal control problem (Patterson and Rao 2014). GPOPS-II is a general-purpose MATLAB software for solving continuous optimal control problems using hp-adaptive Gaussian quadrature collocation method.

Fix  $T = 500$ . We use the default parameter values given in Table 2 and the initial conditions of Table 3 for simulations. The dose of immunotherapy in Fig. 3 follows that of Niu et al. (2013) with  $s = 3.36 \times 10^9$  cells. The results of the three different immunities are given in plots (a)–(c), respectively. The final tumor sizes for these three immunities are  $2.742 \times 10^{10}$ ,  $2.733 \times 10^{10}$  and  $2.731 \times 10^{10}$  cells, respectively, slightly smaller than the critical tumor size of  $2.8 \times 10^{10}$ . The figure shows that the patients with high immunity would need smaller treatment doses. In addition, one sees that a full dose of effector cells is required in the beginning of the treatment and the tumor size is reduced. There is a break of no immunotherapy roughly between 30 and 50 days in which the tumor size increases. The tumor remains increasing when much smaller numbers of effector cells are applied at a later time period. In general, if there is an extra payoff term outside the integral such as  $x(T)$  in the objective functional (3.5), then  $x(t)$  usually decreases at  $t = T$  when  $x$  comes from the left. This is not the case for our model. Although these patients survive for over 500 days, the optimal strategy of the immunotherapy does not seem to be able to control the tumor from growing as in the previous treatment strategies where three or four immunotherapies are applied. We obtain similar numerical results if we change the strength  $s$  of the dose or  $A$  the cost or patient's tolerance of the treatment. These simulations are not presented.

In addition to the optimal solutions, Fig. 3 also shows the plot of tumor cells against time simulated from the clinical implementations of Niu et al. (2013) in which pulsed immunotherapies are carried out on days 1, 30, 59 and 88 only. The protocol derived from the optimal control suggests a continuous administration of immune cells over the first several days. From the figure, we see that the protocol from the optimal control gives a better survival outcome than the pulsed injections of immune cells for four times. However, the total number of immune cells administered using the optimal control is clearly larger than that of the corresponding pulsed treatments.

From this part of the study, we conclude that mono-immunotherapy is not sufficient to control or stabilize pancreatic cancer since the best scheduling and doses of immunotherapies cannot prevent cancer from growing. This particular finding deduced from the optimal control theory is aligned with the current knowledge of PDA described by Martinez-Bosch et al. (2018) and Morrison et al. (2018) in which mono-immunotherapy is not sufficient to control or eradicate pancreatic cancer. This further motivates us to consider combined immunotherapies of anti-TGF- $\beta$  treatments and adoptive cell transfers in the following subsection.

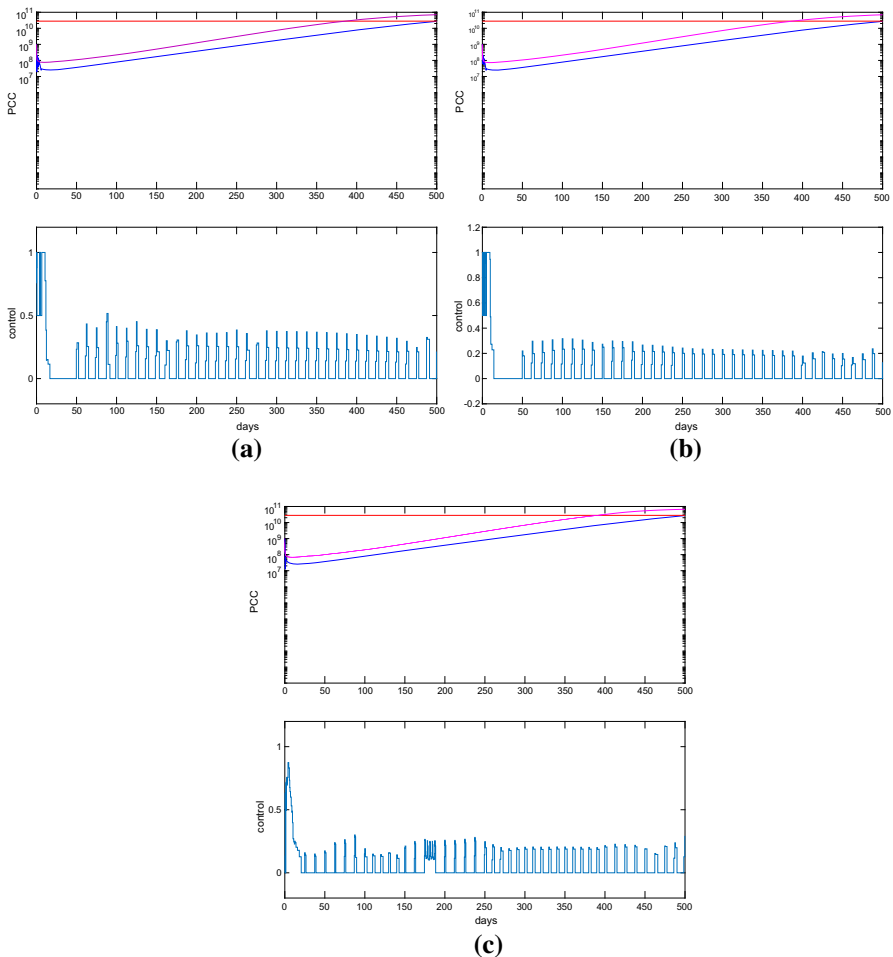


**Fig. 3** Numerical solutions of the optimal immunotherapy and the corresponding tumor size for equations (9)–(12) are plotted (blue solid line) using  $A = 150$  and  $s = 3.36 \times 10^9$  for low, median and high immunities given in (a)–(c), respectively. The solid magenta line denotes tumor evolution resulting from four pulsed immunotherapies, and the top horizontal line is the line of  $2.8 \times 10^{10}$  (Color figure online)

### 3.3 Combined Immunotherapies In Silico

Figure 2 shows that injecting  $3.36 \times 10^9$  effector cells on day one followed by two siRNA treatments or a continuous siRNA treatment starting on day one cannot extend patients' survival compared with four doses of effector cells. This raises the question of the effectiveness of anti-TGF- $\beta$  treatments. Indeed, there is one phase I/II clinical trial of 37 patients using mono-immunotherapy of anti-TGF- $\beta$ , showing no improved survival outcomes except for one patient (Hilmi et al. 2018), who survived for over two years and may be considered as an outlier. However, our sensitivity analysis performed in “Appendix” does reveal that reducing activation rate of pro-tumor cytokines before

applying immunotherapies can kill cancer cells completely. In this subsection, we study different combinations of therapies using numerical simulations.

Since deactivating pro-tumor cytokines prior to adoptive cell transfers seems critical, an siRNA treatment is now applied on day one for 11 days followed by 28 days of no treatment. Then, three injections of  $3.36 \times 10^9$  effector cells are applied with 28 days of no immunotherapy in between. The result is given in Fig. 4a. After the first 11 days of siRNA treatment, we see that the tumor grows slightly larger than the continuous siRNA treatment over the period of first 28 days of no treatment. However, as the effector cells are applied on day 40, the tumor size is slightly smaller than for the immunotherapies applied on day one and on day 30. The tumor size remains smaller than the three immunotherapies of adoptive transfer of immune cells, which may be due to the extra siRNA treatment received. We apply a similar strategy with four applications of  $3.36 \times 10^9$  ex vivo expanded immune cells and obtain a similar numerical result with respect to tumor size as shown in Fig. 4b. We next change the strategy by using one more siRNA treatment instead of adoptive cells and are able to reduce the tumor size more substantially as shown in Fig. 4c. Here, the siRNA treatment is applied on day one followed by two injections of effector cells and then one more siRNA treatment. Each of the siRNA treatment lasts for 11 days, and there are 28 days of no treatment between any of the successive therapies. We see that this later combination of treatments gives a better survival outcome.

Recall from an earlier discussion that the immunotherapies applied to patients by Niu et al. (2013) are more conservative than those by Chung et al. (2014). In fact, the dosage of the effector cells in Niu et al. (2013) is  $3.36 \times 10^9$  cells, while it is  $6.73 \times 10^9$  cells in Chung et al. (2014). In addition, only four immunotherapies are applied in Niu et al. (2013) while the patients of Chung et al. (2014) receive either seven, eight or ten doses of immune cells and the break between treatments in Chung et al. (2014) is much shorter than that in Niu et al. (2013). Although the patients of Niu et al. received cryotherapy prior to immunotherapy, these patients in Chung et al. also underwent chemotherapy before immunotherapy. The strategy of Niu et al. (2013) is adopted in Figs. 2 and 4, where the number of effects cells is  $3.36 \times 10^9$  and there is a 28-day break between treatment. Further, at most four doses of effector cells are applied.

We now apply the clinical practice of Chung et al. (2014) with doses of  $6.73 \times 10^9$  cells and a one-week break between any two consecutive treatments to study patient survival. In order to compare with these strategies in Figs. 2 and 4, the median immunity is used for Figs. 5 and 6. First, we apply two siRNA treatments and four injections of ex vivo expanded immune cells. Each siRNA treatment lasts for only a week instead of 11 days, and each injection of immune cells is within a day. These results are presented in Fig. 5 with three different combinations. The red dash-dot line adopts the strategy of applying siRNA treatment in the first week followed by injection of effector cells three times. Then, one more siRNA treatment is applied followed by one more injection of effector cells. The black dotted line represents siRNA treatment for the first week followed by one injection of effector cells. Then, an siRNA treatment is applied followed by three injections of effector cells. The blue dashed line denotes that two consecutive siRNA treatments are applied first followed by injections of effector cells four times. Figure 5b shows the plot of tumor size of these three strategies for the first 60 days. One can see that applying siRNA treatment first followed by one

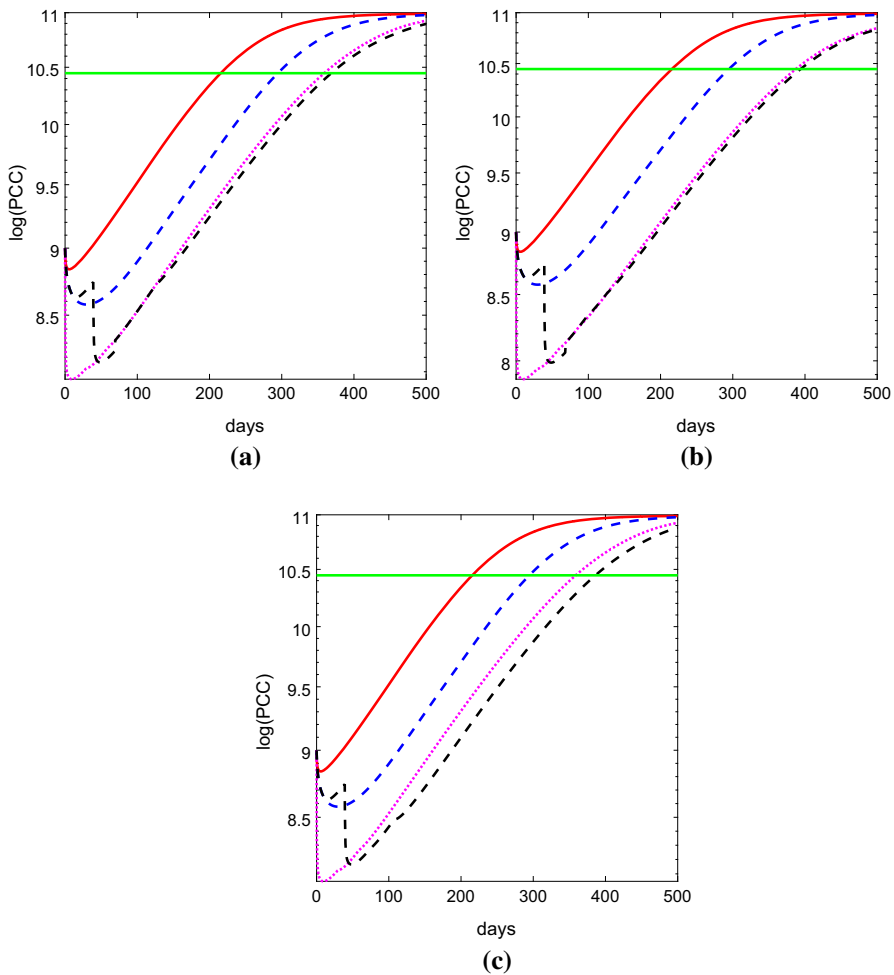


**Fig. 4** Baseline parameter values in Table 2 and the median immunity in Table 3 are used for the simulations. Each of the red solid lines represents no immunotherapy, while continuous siRNA treatment is plotted by blue dashed lines. **a** Three injections of effector cells (magenta dotted line) or first anti-TGF- $\beta$  followed by three injections of effector cells (black dashed line). **b** Four injections of effector cells (magenta dotted line) or first anti-TGF- $\beta$  followed by four injections of effector cells (black dashed line). **c** Four injections of effector cells (magenta dotted line) or first anti-TGF- $\beta$  followed by two additional injections of effector cells and one more anti-TGF- $\beta$  treatment (black dashed line). There is a 28-day break between any successive treatments. The parameter values of siRNA treatment are given in (8), and the number of each adoptive cell transfer consists of  $3.36 \times 10^9$  cells. The PCCs are scaled by a common logarithm, and the top horizontal line is the scaled line of  $2.8 \times 10^{10}$  (Color figure online)

injection of effector cells and then an anti-TGF- $\beta$  is better than the other two options. However, its benefit becomes smaller after 100 days since the treatment period only lasts for about 50 days.

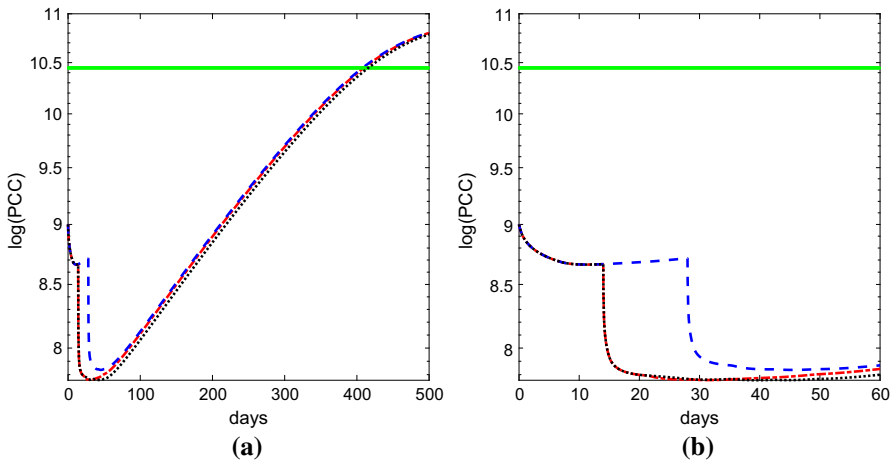


**Fig. 5** Baseline parameter values in Table 2 and the median immunity in Table 3 are used. The parameter values of siRNA treatment are given in (8), and the number of each injection of effector cells is  $6.73 \times 10^9$ . The break between any two consecutive treatments is one week. **a** Three different treatment strategies are shown. Red dash-dot line: first week of siRNA treatment followed by injection of effector cells three times. Then, one more siRNA treatment is applied followed by one more injection of effector cells. Black dotted line: first week of siRNA treatment followed by one injection of effector cells. Then, an siRNA treatment is applied followed by three injections of effector cells. Blue dashed line: two consecutive siRNA treatments that are applied first followed by injections of effector cells four times. **b** A closer look of plot (a) for the first 60 days. The PCCs are scaled by a common logarithm and the top horizontal line is the scaled line of  $2.8 \times 10^{10}$  (Color figure online)

In Fig. 6, we apply siRNA treatment first followed by immunotherapy of effector cells. We repeat this strategy for three times followed by two additional immunotherapies, denoted by the red dash-dot line. Totally there are three siRNA treatments and five times of adoptive cell transfers. The treatment of the blue dotted line is similar to the red dash-dot line but replaces the second last injection of effector cells by an siRNA treatment. Therefore, there are four siRNA treatments and four adoptive cell transfers. Figure 6b shows that the first treatment strategy is doing better during the time interval of about 65 to 80 days. However, the second treatment strategy can extend patients’ life at the end as shown in plot (c).

### 4 Summary and Conclusions

Pancreatic ductal adenocarcinoma (PDA) is a deadly disease with the lowest 5-year patient survival rate of any tumor type. The incidence of PDA is rising, and it is projected to become the second leading cause of cancer death in the USA by 2025 (Winograd et al. 2015). In the last few decades, immunotherapy has become an important tool for treating cancer of different types with varying degree of success. However, this efficacy has not yet been translated to PDA (Morrison et al. 2018).

In this study, we develop a mathematical model of PDA that includes pancreatic cancer cells (PCCs), pancreatic stellate cells (PSCs), effector cells, and anti-tumor

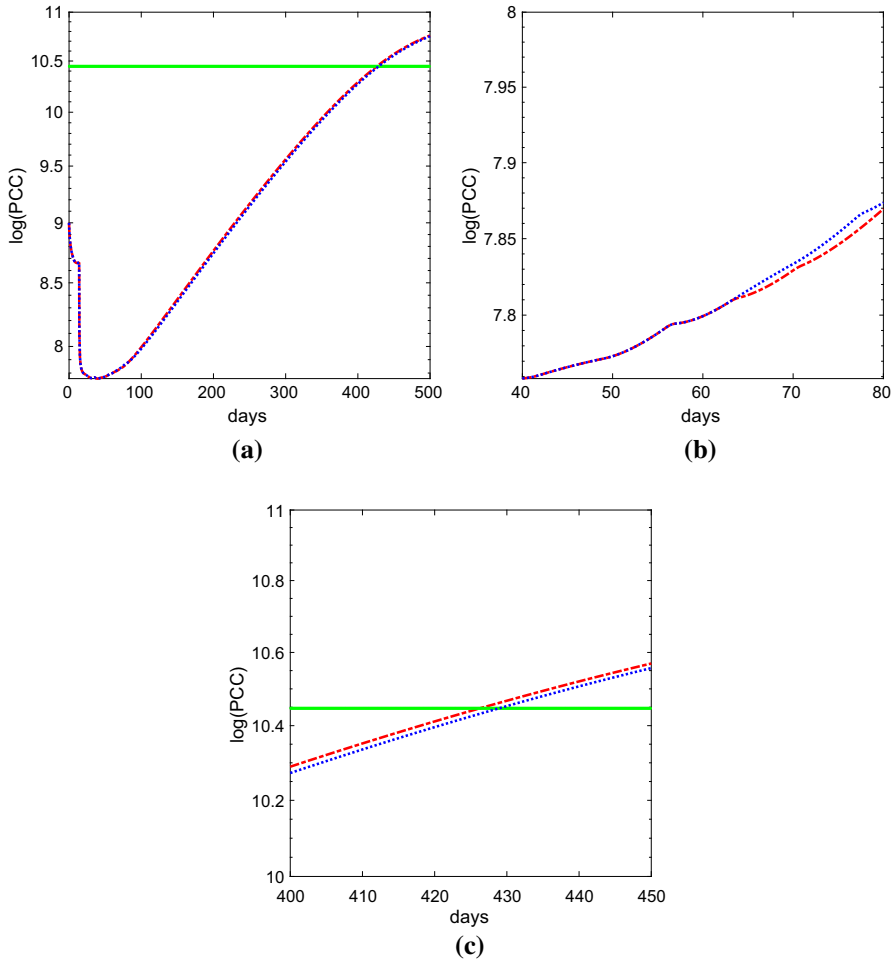
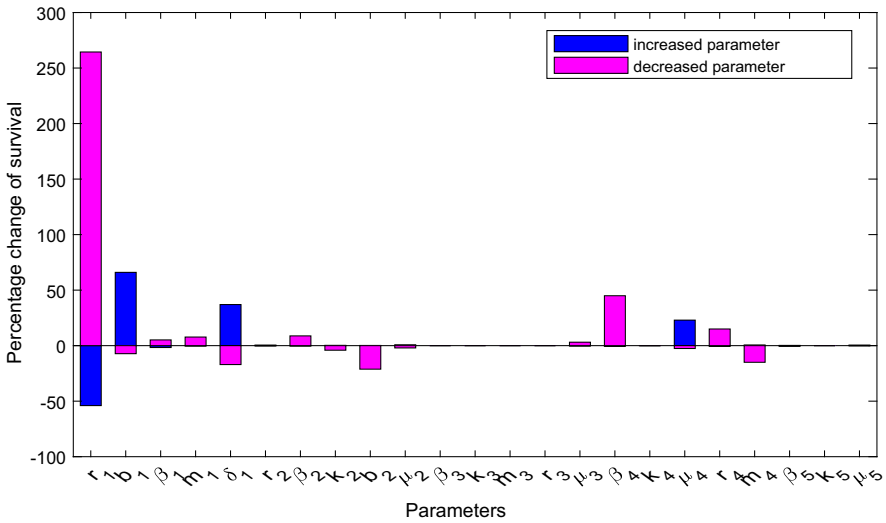


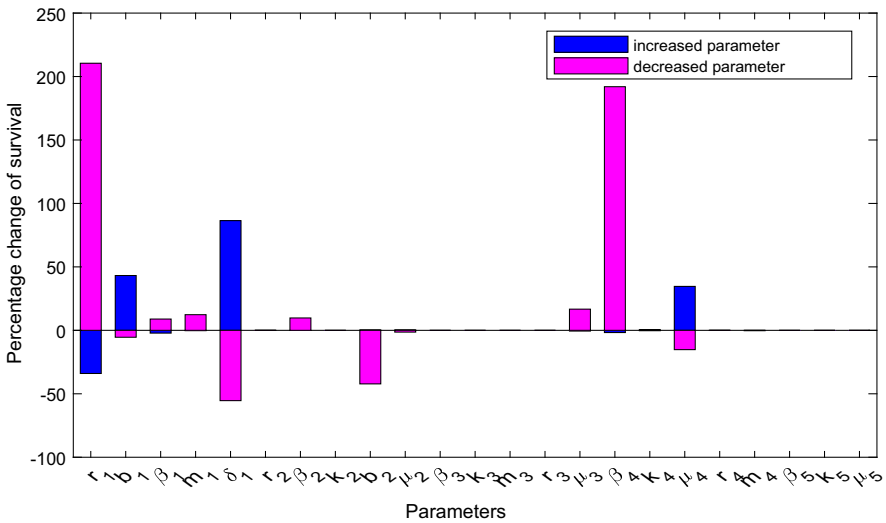
**Fig. 6** Baseline parameter values in Table 2 and the median immunity in Table 3 are used. The parameter values of siRNA treatment are given in (8), and the number of each injection of effector cells is  $6.73 \times 10^9$ . The break between any two consecutive treatments is one week. **a** Two different treatment strategies are shown. Red dash-dot line: first week of siRNA treatment followed by one injection of effector cells and repeat this strategy for two additional times followed by two more injections of effector cells. Blue dotted line: similar to the red dash-dot line except the last second treatment of effector cells is replaced by an siRNA treatment. **b** Solutions of (a) when  $t \in [40, 80]$  days. **c** Solution of (a) when  $t \in [400, 450]$  days. The PCCs are scaled by a common logarithm, and the top horizontal line is the scaled line of  $2.8 \times 10^{10}$  (Color figure online)

and pro-tumor cytokines to explore the effects of immunotherapies, including TGF- $\beta$  inhibition and adoptive immune cell transfers, on patients survival. One of the novelties of the proposed model is that tumor-promoting and tumor-suppressing cytokines are grouped into two compartments and their productions are modeled via the Michaelis–Menten law. Further, as pro-tumor cytokines are not only triggered by the interaction between PCCs and effector cells but are also activated by cross talk between cancer





(a)



(b)

**Fig. 7** Relative maximal percentage of changes in the baseline parameters to patient’s survival are plotted. There is no immunotherapy in **a** and patients receive four adoptive transfers of  $3.36 \times 10^9$  cells in **b**. The median immunity in Table 3 is used for the simulations (Color figure online)

cells and stellate cells (Kozono et al. 2013), we model this positive feedback in the present investigation as well. These assumptions are different from the previous models of pancreatic cancer (Louzoun et al. 2014; Li and Xu 2016; He and Xu 2017). In addition, pro-tumor cytokines can deactivate effector cells and inhibit their ability to

kill tumor cells, and these mechanisms are not modeled in Li and Xu (2016) and He and Xu (2017).

The proposed model is first validated using two clinical data sets provided by Niu et al. (2013) and Chung et al. (2014). Based on the survival data of Niu et al. (2013), the maximum percentage that each individual parameter can deviate from the baseline value is computed for both cases of no immunotherapy and of four immunotherapies. From here, we learn that the activation rate of pro-tumor cytokines plays a critical role in tumor eradication when adoptive transfers of immune cells are applied.

Louzoun et al. (2014) validate their mathematical model using the mouse survival data of Ellermeier et al. (2013). Although anti-TGF- $\beta$  in the mouse model of Ellermeier et al. (2013) is through siRNA treatments, the siRNA treatment in Louzoun et al. (2014) is not explicitly modeled but the TGF- $\beta$  inhibition is done by reducing several parameter values directly from their baseline values. In this investigation, we model the siRNA treatment explicitly with a new state variable that is coupled with pro-tumor cytokines. We are able to accomplish this, due to the fact that we do not take the quasi-steady-state approximation approach as in Louzoun et al. (2014), Li and Xu (2016) and He and Xu (2017). Moreover, since no model reduction is taken in this study, we are able to investigate the effects of different combined therapies between anti-TGF- $\beta$  and adoptive transfers of immune cells on patient survival.

The model of Louzoun et al. (2014) includes macrophages, and, similar to the anti-TGF- $\beta$  modeling, the immune activation is also modeled through varying several parameter values. Their study predicts that immunotherapy is effective when the tumor killing rate by effector cells is within a narrow range, which is the window of opportunity for combating PDA. While Li and Xu (2016) model the adoptive cell transfers explicitly, they do not consider anti-TGF- $\beta$  treatment. The study by Li and Xu (2016) concludes that immunotherapy offers a better prognosis for pancreatic cancer patients since the therapy can prolong survival compared with no immunotherapy. Their simulations also show a continuous growth of tumor size with treatments of adoptive transfers of immune cells. In a more recent model proposed by He and Xu (2017), regulatory T cells (Tregs) and anti-Tregs therapy are included. They predict that the combined therapies of adoptive cell transfer and anti-Tregs simultaneously can prolong patients' survival. However, the growing pattern of pancreatic cancer cannot be stopped or reversed even with the two therapies.

The immune activation in this work is modeled explicitly through intravenous injections of immune cells. Combined immunotherapies between adoptive transfer of immune cells and anti-TGF- $\beta$  are also studied, but are not simultaneously implemented as in He and Xu (2017) for the two agents. From numerical explorations of this new model, we find that different combinations between the two types of immunotherapies can yield different survival outcomes, indicating the importance of treatment strategies. In addition, local sensitivity analysis of the parameters shows that pro-tumor cytokines have a critical activation rate beyond which the PCCs can be eradicated with only four adoptive transfers of immune cells. Applying anti-TGF- $\beta$  therapy first followed by adoptive transfer of immune cells can reduce the tumor load better than if this combination were switched or if either of the mono-immunotherapies were applied. The microenvironment of PDA is very immunosuppressive. By deactivating TGF- $\beta$  production first followed by adoptive transfer of immune cells, the

microenvironment is less hostile for the immune cells to be effective. We confirm from optimal control theory that mono-immunotherapy of adoptive cell transfer is unlikely to control PDA. This study further highlights the importance of combined immunotherapies and their scheduling strategies in treating pancreatic cancer.

Blockade of immune checkpoints has recently been proven as a revolutionary strategy in the fight against cancers. The success of these therapies has failed to improve the survival outcome of patients in PDA (Martinez-Bosch et al. 2018; Morrison et al. 2018). According to Winograd et al. (2015), clinical trials using either single agent of anti-CTLA-4 or combined agents of anti-CTLA-4 and anti-PD-1 show no improved patient survival, while the two combined immunotherapies along with chemotherapy have been shown to induce tumor rejection in a genetically engineered PDA murine model. However, the success in murine models may not carry over to patients as illustrated in several experiments and clinical studies of PDA (Martinez-Bosch et al. 2018; Morrison et al. 2018). Anti-PD-1 has recently been incorporated into a generic cancer model of partial differential equations by Friedman and Hao (2017). We may extend the present mathematical model (6) by adding compartments of CTLA-4 and PD-1 with their ligands and studying their blockades in addition to chemotherapy on patients to explore their effects on patient survival.

**Acknowledgements** We thank both reviewers for their many valuable comments that improved the original manuscript.

## Appendix: Sensitivity Analysis Based on the Survival Data of Niu et al.

From Fig. 1a of Niu et al. (2013), there is one patient who survived for about 25 months with no immunotherapy and there is one patient who survived for about 30 months with four additional immunotherapies. For both groups of patients, there is one patient who survived for only about three months. These survival times are not outliers of the data sets, and there are no numerical values for the mean and standard deviation given by Niu et al. (2013). If such information were provided, then change in the parameter values based on a 90% or 95% confidence interval of the clinical data would be performed instead. We therefore increase each individual parameter by up to 3000% or until the survival time lies outside of (120, 750) days for cryotherapy and (120, 900) days for cryo-immunotherapy. For both groups of patients, only the median immunity is considered in our numerical investigation. We also decrease each baseline parameter value until either up to 90% or the survival time falls outside of the above time intervals. These results are summarized in Tables 5 and 6 for cryotherapy and cryo-immunotherapy, respectively. In addition, the numbers of survival days for the corresponding maximum percentage of changes are also provided.

From Table 5, one can see that parameters  $\beta_3$ ,  $k_3$ ,  $m_3$ ,  $r_3$ ,  $k_4$ ,  $k_5$  and  $\mu_5$  can be increased up to 3000% and decreased up to 90% without changing the survival time of 215 days from the baseline parameters when no immunotherapy is applied. It is quite surprising to observe the lack of effect of parameter  $\beta_3$  since  $\beta_3$  is the tumor antigenicity. Increasing/decreasing tumor antigenicity cannot prolong/reduce a patient's survival time in the proposed model when there is no immunotherapy. For the tumor

**Table 5** Maximum percentage of change from baseline parameter values with no immunotherapy for median immune strength

Parameter	Increase (%)	Survival (days)	Decrease (%)	Survival (days)
$r_1$	80	122	70	613
$b_1$	250	568	90	201
$\beta_1$	2000	140	90	225
$m_1$	3000	195	90	230
$\delta_1$	400	529	90	182
$r_2$	3000	206	90	216
$\beta_2$	3000	195	90	232
$k_2$	3000	233	90	207
$b_2$	3000	227	90	174
$\mu_2$	3000	266	90	211
$\beta_3$	3000	215	90	215
$k_3$	3000	215	90	215
$m_3$	3000	215	90	215
$r_3$	3000	215	90	215
$\mu_3$	3000	196	90	221
$\beta_4$	3000	178	90	302
$k_4$	3000	216	90	215
$\mu_4$	1000	709	90	210
$r_4$	3000	178	90	245
$m_4$	3000	255	90	186
$\beta_5$	3000	229	90	214
$k_5$	3000	215	90	215
$\mu_5$	3000	214	90	216

The corresponding survival time for the baseline values is 215 days

killing rate  $\delta_1$ , it can be increased only up to 400% with the corresponding survival time being 529 days. Increasing  $\delta_1$  further would result in tumor eradication since the number of cancer cell would be less than one. It is also clear that the survival time is sensitive with respect to two other parameters  $r_1$  and  $b_1$  which are tumor dependent. Increasing  $b_1$  or decreasing  $r_1$  beyond the percentage changes given in the table also results in tumor eradication. Further, the survival time is sensitive to the parameter  $\mu_4$ , the decay rate of the pro-tumor cytokines. Increasing this natural loss rate can clear off the tumor.

With four immunotherapies, the survival time is 387 days for the baseline parameter values with median immunity. Table 6 implies that the survival time is insensitive to the parameters  $\beta_3, k_3, m_3, r_3, m_4, \beta_5, k_5$  and  $\mu_5$  since increasing each of these up to 3000% or decreasing each up to 90% yields the same number 387 of survival days. Comparing with the above discussion of Table 5 of no immunotherapies, there are two

**Table 6** Maximum percentage of change from baseline parameter values with four immunotherapies for median immune strength

Parameter	Increase (%)	Survival (days)	Decrease (%)	Survival (days)
$r_1$	200	124	55	835
$b_1$	250	805	90	368
$\beta_1$	3000	131	90	418
$m_1$	3000	356	90	430
$\delta_1$	110	755	90	194
$r_2$	3000	384	90	387
$\beta_2$	3000	379	90	421
$k_2$	3000	387	90	387
$b_2$	3000	420	90	240
$\mu_2$	3000	422	90	382
$\beta_3$	3000	387	90	387
$k_3$	3000	387	90	387
$m_3$	3000	387	90	387
$r_3$	3000	387	90	387
$\mu_3$	3000	320	90	445
$\beta_4$	3000	184	55	796
$k_4$	3000	444	90	386
$\mu_4$	250	722	90	334
$r_4$	3000	383	90	387
$m_4$	3000	387	90	386
$\beta_5$	3000	387	90	387
$k_5$	3000	387	90	387
$\mu_5$	3000	387	90	387

The corresponding survival time for the baseline values is 387 days

new parameters  $m_4$  and  $\beta_5$  that appear here. However, their corresponding changes in Table 5 are very small which can also be viewed as insensitive when there is no immunotherapy. The survival time is sensitive to the parameters  $\delta_1$ ,  $r_1$ ,  $b_1$ ,  $\mu_4$  and  $\beta_4$ . The first four of these parameters are also sensitive to the survival time when there is no immunotherapy. The additional parameter  $\beta_4$ , the maximum activation rate of pro-tumor cytokines, is sensitive when immunotherapy is applied. In particular, the number of tumor cells is less than one and tumor eradication occurs when it is decreased 60% from its baseline value.

Since bar charts provide better visualization of the effects on survival time, we also summarize the two tables using graphs presented in Fig. 7a–b, respectively. However, it is unclear how much each individual parameter can be varied from the bar graphs, and hence, Tables 5 and 6 are also provided to reflect the maximum percentages of changes and their corresponding survival times.

## References

- Abdo J et al (2018) Immunotherapy plus cryotherapy: potential augmented abscopal effect for advanced cancers. *Front Oncol* 8:1–16
- Anderson L, Jang SR-J, Yu J (2015) Qualitative behavior of systems of tumor-CD4<sup>+</sup>-cytokine interactions with treatments. *Math Methods Appl Sci* 38:4330–4344
- Arciero JC, Jackson TL, Kirschner DF (2004) A mathematical model of tumor-immune evasion and siRNA treatment. *Dis Cont Dyn Syst Ser B* 4(1):39–58
- Bachem MG et al (2008) Pancreatic stellate cells role in pancreas cancer. *Langenbecks Arch Surg* 393:891–900
- Bellone et al (2006) Cytokine expression profile in human pancreatic carcinoma cells and in surgical specimens: implications for survival. *Cancer Immunol Immunother* 55:684–698
- Burden T, Ernstberger J, Fister K (2004) Optimal control applied to immunotherapy. *Dis Cont Dyn Sys Ser B* 4:135–146
- Castiglione F, Piccoli B (2007) Cancer immunotherapy, mathematical modeling and optimal control. *J Theor Biol* 247:723–732
- Chung MJ et al (2014) Phase II clinical trial of ex vivo-expanded cytokine-induced killer cells therapy in advanced pancreatic cancer. *Cancer Immunol Immunother* 63(9):939–946
- de Pillis L et al (2005) A validated mathematical model of cell-mediated immune response to tumor growth. *Cancer Res* 65(17):7950–7958
- de Pillis L et al (2008) Optimal control of mixed immunotherapy and chemotherapy of tumors. *J Biol Syst* 16(1):51–80
- Diefenbach A et al (2001) Rae1 and H60 ligands of the NKG2D receptor stimulate tumor immunity. *Nature* 413:165–171
- Eftimie R et al (2010) Anti-tumour Th1 and Th2 immunity in the rejection of melanoma. *J Theor Biol* 265:467–480
- Ellermeier J et al (2013) Therapeutic efficacy of bifunctional siRNA combining TGF- $\beta$ 1 silencing with RIG-I activation in pancreatic cancer. *Cancer Res* 73(6):1709–1720
- Engelhart M, Lebiezd D, Sager D (2011) Optimal control for selected cancer chemotherapy ODE models: a view on the potential of optimal schedules and choice of objective function. *Math Biosci* 229:123–134
- Fire A et al (1998) Potent and specific genetic interference by double-stranded RNA in *Caenorhabditis elegans*. *Nature* 391:806–811
- Fleming W, Rishel R (1975) *Deterministic and stochastic optimal control*. Springer, New York
- Friedman A, Hao W (2017) The role of exosomes in pancreatic cancer microenvironment. *Bull Math Biol* 79:1–23
- Friedman A, Lai X (2018) Combination therapy for cancer with oncolytic virus and checkpoint inhibitor: a mathematical model. *PLoS One* 13(2):1–21
- Gaspar NJ et al (2007) Inhibition of transforming growth factor beta signaling reduces pancreatic adenocarcinoma growth and invasiveness. *Mol Pharmacol* 72:152–161
- Gold L (1999) The role for transforming growth factor- $\beta$  (TGF- $\beta$ ) in human cancer. *Crit Rev Oncog* 10:303–360
- Hanahan D, Weinberg RA (2011) Hallmarks of cancer: the next generation. *Cell* 144:646–674
- Hariharan D et al (2008) Analysis of mortality rates for pancreatic cancer across the world. *HPB* 10:58–62
- He D-H, Xu J-X (2017) A mathematical model of pancreatic cancer with two kinds of treatments. *J Biol Syst* 25(1):83–104
- Heinemann V (2001) Gemcitabine: progress in the treatment of pancreatic cancer. *Oncology* 60(1):8–18
- Hilmi M et al (2018) Immune therapies in pancreatic ductal adenocarcinoma: where are we now? *World J Gastroent* 24(20):2137–2151
- Holen T et al (2001) Positional effects of short interfering RNAs targeting the human coagulation trigger tissue factor. *Nucleic Acids Res* 30:1757–1766
- Hu X, Jang SR-J (2018a) Dynamics of tumor-CD4<sup>+</sup>-cytokine-host cells interactions with treatments. *Appl Math Comput* 321:700–720
- Hu X, Jang SR-J (2018b) Optimal treatments in cancer immunotherapy involving CD4<sup>+</sup> T cells. *WSEAS Trans Biol Biomed* 15:48–67
- Khajanchi S, Ghosh D (2015) The combined effects of optimal control in cancer remission. *Appl Math Compu* 271:375–388

- Kirschner D, Panetta JC (1998) Modeling immunotherapy of the tumor-immune interaction. *J Math Biol* 37:235–252
- Korobeinikov A et al (2016) Paradox of enrichment and system order reduction: bacteriophages dynamics as case study. *Math Med. Biol* 33:359–369
- Kozono S et al (2013) Pirfenidone inhibits pancreatic cancer desmoplasia by regulating stellate cells. *Cancer Res* 73(7):2345–2356
- Kuznetsov V et al (1994) Nonlinear dynamics of immunogenic tumors: parameter estimation and global bifurcation analysis. *Bull Math Biol* 56(2):295–321
- Lenhart L, Workman JT (2007) Optimal control applied to biological models. Chapman & Hall, New York
- Li X, Xu J-X (2016) A mathematical prognosis model for pancreatic patients receiving immunotherapy. *J Theor Biol* 406:42–51
- Lipardi C et al (2001) RNAi as random degradative PCR: siRNA primers convert mRNA into dsRNAs that are degraded to generate new siRNAs. *Cell* 107:297–307
- Louzoun Y et al (2014) A mathematical model for pancreatic cancer growth and treatments. *J Theor Biol* 351:74–82
- Luo X et al (2016) Advances in cryoablation for pancreatic cancer. *World J Gastroenterol* 22(2):790–800
- Mace TA et al (2013) Pancreatic cancer associated stellate cells promote differentiation of myeloid-derived suppressor cells in a stat3-dependent manner. *Cancer Res* 73:3007–3018
- Martinez-Bosch N et al (2018) Immune evasion in pancreatic cancer: from mechanisms to therapy. *Cancers* 10(6):1–16
- Maloney E et al (2017) Focused ultrasound for immuno-adjuvant treatment of pancreatic cancer: an emerging clinical paradigm in the era of personalized oncotherapy. *Int Rev Immunol* 36(6):338–351
- Minelli A et al (2011) Controlled drug delivery in cancer immunotherapy: stability, optimization, and Monte Carlo analysis. *SIAM J Appl Math* 71:2220–2245
- Morrison A et al (2018) Immunotherapy and prevention of pancreatic cancer. *Trends Cancer* 4(6):418–428
- Nam JS et al (2008) Transforming growth factor beta subverts the immune system into directly promoting tumor growth through interleukin-17. *Cancer Res* 68(10):3915–3923
- Niu L et al (2013) Combination treatment with comprehensive cryoablation and immunotherapy in metastatic pancreatic cancer. *Pancreas* 42:1143–1149
- Patterson MA, Rao AV (2014) GPOPS-II: a MATLAB software for solving multiple-phase optimal control problems using hp-adaptive Gaussian quadrature collocation methods and sparse nonlinear programming. *ACM Trans Math Softw* 41(1):1–37
- Rahib L et al (2014) Projecting cancer incidence and deaths to 2030: the unexpected burden of thyroid, liver, and pancreas cancers in the United States. *Cancer Res* 74(11):2913–2921
- Siu H et al (1986) Tumor dormancy. I. Regression of BCL tumor and induction of a dormant tumor state in mice chimeric at the major histocompatibility complex. *J Immunol* 137:1376–1382
- Weinberg RA (2013) The biology of cancer, 2nd edn. Garland Science, London
- Winograd R et al (2015) Induction of T-cell immunity overcomes complete resistance to PD-1 and CTLA-4 blockade and improves survival in pancreatic carcinoma. *Cancer Immunol Res* 3(4):399–411
- Xu C, Wang J (2015) Delivery systems for siRNA drug development in cancer therapy. *Asian J Pharm Sci* 10:1–12
- Xue H et al (2016) A novel tumor-promoting mechanism of IL-6 and the therapeutic efficacy of tocilizumab: Hypoxia-induced IL-6 is a potent autophagy initiator in glioblastoma via the p-STAT3-MIR155-3p-CREBRF pathway. *Autophagy* 12:1129–1152
- Yates A, Callard R (2002) Cell death and the maintenance of immunological memory. *Discrete Contin Dyn Syst Ser B* 1(1):43–59
- Zhao J et al (2016) Clinical and prognostic significance of serum transforming growth factor- $\beta$  1 levels in patients with pancreatic ductal adenocarcinoma. *Br J Med Biol Res* 49(8):1–5